This article has been accepted for publication in a future issue of this journal, but has not been fully edited. Content may change prior to final publication. Citation information: DOI 10.1109/LAWP.2014.2363596, IEEE Antennas and Wireless Propagation Letters

Design and Performance Evaluation of a Dielectric Flat Lens Antenna for Millimeter-Wave Applications

Marc Imbert, *Student Member, IEEE*, Anna Papió, *Student Member, IEEE*, Franco De Flaviis, *Fellow, IEEE*, Lluís Jofre, *Fellow, IEEE*, and Jordi Romeu, *Fellow, IEEE*

***Abstract*—In this paper, a practical fabrication of a novel inhomogeneous gradient-index dielectric flat lens for millimeter-wave applications is presented. A previous theoretical design of a dielectric flat lens composed of different permittivity materials is now modeled and analyzed for a practical prototype fabrication and performance evaluation at 60 and 77 GHz. The measurement results at 60 GHz show that with the novel gradient-index dielectric flat lens antenna prototype we can achieve up to 18.3 dB of broadside gain, beam-steering capabilities in both planes from -30º to +30º with around 15 dB of gain, and up to ±45º with around 14 dB of gain, with low side-lobe levels. At 77 GHz, the performance evaluation shows that we can obtain up to 18.9 dB of broadside gain, beam-steering capabilities in both planes from -30º to +30º with around 17 dB of gain and low side-low levels, and up to ±45º with around 15 dB of gain. This novel design leads to a low-cost, low-profile and lightweight antenna solution, easy to integrate in a compact millimeter-wave wireless communication system.**

***Index Terms*—Automotive radar applications, beam-steering, flat lens antenna, millimeter-wave, switched-beam array, WPAN.**

I. Introduction

In recent years, the scientific community and the industry have focused their attention on different frequency bands that could satisfy the increasing bandwidth requirements of modern communication systems. Given the large amount of available bandwidth, the millimeter-wave frequency band represents one of the most interesting candidates. However, in accordance with the Friis transmission formula, the path loss in free-space propagation is much higher at millimeter-wave frequencies than at lower microwave frequencies (e.g. the path loss at 60 GHz is 28 dB higher than at 2.45 GHz). In consequence, millimeter-wave systems introduce a set of particular severe requirements from the antenna point of view.

Manuscript submitted on May 22, 2014. This work was supported in part by the Spanish Inter-Ministerial Commission on Science and Technology (CICYT) under the projects TEC2010-20841-C04-02, TEC2013-47360-C3-1-P and CONSOLIDER CSD2008-00068, by the "Ministerio de Economía y Competitividad" through the FPI Fellowship Program, and by the California-Catalonia Engineering Innovation Program.

Marc Imbert, Jordi Romeu and Lluís Jofre are with AntennaLab Research Group at Department of Signal Theory and Communications from the Universitat Politècnica de Catalunya (UPC), 08034, Barcelona, Spain (e-mail: marc.imbert@tsc.upc.edu).

Anna Papió and Franco De Flaviis are with the Department of Electrical Engineering and Computer Science, University of California at Irvine (UCI), Irvine, CA, 92697-7625, USA (email: apapioto@uci.edu).

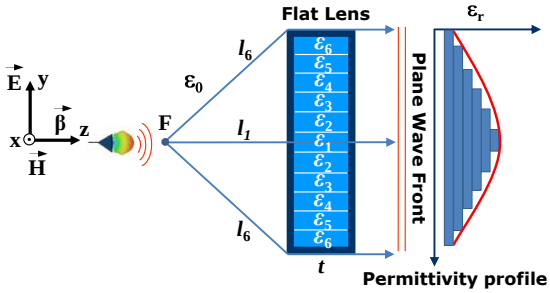

Fig. 1. Dielectric flat lens antenna functioning principle.

Therefore, high directive antennas are required to overcome the aforementioned extra path loss. Moreover, each particular application introduces additional requirements. For example, in very high throughput 60 GHz band (from 57 to 64 GHz in the Unites States) [1] wireless personal area networks (WPANs) beam-steering antennas are needed to deal with the high user random mobility and human-body shadowing characteristic of indoor environments [2]. Similarly, beam-steering capabilities are also needed in automotive radar applications at 77 GHz [3], since the determination of the exact position of an object is essential for most of the functions performed by the radar sensor. Finally, the antennas must be small, low-profile, lightweight and low-cost, in order to be successfully integrated in a commercial wireless system.

Many types of antenna structures are considered for short-range 60 GHz WPAN applications [2], and for automotive radar applications at 77 GHz [3], most of them based on the expensive, complex and bulky phased-array antenna concept. Switched-beam arrays provide an interesting alternative because they have multiple fixed beams that can be easily selected individually, and the implementation is much easier than phased-array antennas. For these reasons, in [4] we proposed a design based on a switched-beam array antenna concept with a theoretical design of an inhomogeneous dielectric flat lens modeled with different materials to steer and enhance the radiation in a particular direction. In this antenna concept, only one element of the array is selected for each operation mode. The focusing direction depends on the position of the single element, which is selected and activated [4]. In this sense, different types of inhomogeneous (multi-material or gradient-index) lenses have been proposed in the literature [5-10]. Fresnel zone plate lenses [5] are widely used to correct the phase of the feed antenna; however, this correction is performed only at discrete locations, leading to an

This article has been accepted for publication in a future issue of this journal, but has not been fully edited. Content may change prior to final publication. Citation information: DOI 10.1109/LAWP.2014.2363596, IEEE Antennas and Wireless Propagation Letters

TABLE I. PERFORATED DIELECTRIC FLAT LENS CHARACTERISTIC PARAMETERS

Ring	Ring width	ε_{reff}	α	d	s
1	1.14 mm	6.05	-	-	-
2	2.27 mm	5.77	0.06	0.2 mm	0.81 mm
3	2.27 mm	5.06	0.2	0.5 mm	1.08 mm
4	2.27 mm	4.13	0.38	0.5 mm	0.77 mm
5	2.27 mm	3.16	0.57	0.5 mm	0.63 mm
6	2.27 mm	2.25	0.75	0.5 mm	0.55 mm

inherently narrowband behavior. Luneburg lenses [6-9] are an interesting alternative of spherical or hemispherical gradient-index lenses because of their very good performance; however, their planar implementations allow beam-scanning in only one plane.

In this paper, we present the practical fabrication and performance evaluation of a novel inhomogeneous gradient-index dielectric flat lens antenna for millimeter-wave applications based on the concept of our previous theoretical work [4]. Its performance is evaluated at 60 and 77 GHz. The proposed antenna solution is very attractive because represents an innovative alternative to the existing antenna configurations at millimeter-wave frequencies to achieve beam-scanning in both planes while keeping at the same time a flat antenna profile, much thinner than conventional existing shaped lenses, with broadband operation.

II. LENS DESIGN AND SIMULATION RESULTS

The dielectric flat lens operating principle is shown in Fig. 1, and the first stage of the design procedure is described in [4]. The theoretical lens design introduced in [4] consists of a set of six concentric rings of different permittivity (εr) materials, in order to produce the desired phase delays required to obtain a plane wave behind the lens, when the lens is illuminated from its central focus position. In the same way, when the feeding position is moved along y-direction (see Fig. 1) the different permittivity values of the lens produce a linear phase slope that steers the beam, accordingly [4].

A. Practical Dielectric Flat Gradient-Index Lens Design

Alternative methods should be investigated because of the difficulty of fabricating lenses through the fusion of different permittivity materials. For example, the relative permittivity of a dielectric substrate material can be reduced by perforating a single layer of substrate [5]-[6]. If the diameter of holes (d) and the distance between holes (s) are kept small compared to the wavelength of operation, the substrate will appear to have a uniform effective permittivity. Therefore, we modeled, analyzed, and optimized the theoretical lens in order to design and fabricate a prototype from a single layer of perforated dielectric material. The final diameter of the lens was reduced to D=25 mm ($5\lambda_{60GHz}$), with a focal length of F=D/4, and a thickness of 7 mm ($1.4\lambda_{60GHz}$). Moreover, we optimized the design to lower the effective permittivity values required to avoid the considerable reflections that could occur between the radiating elements and the lens (due to the change of media). Then, the maximum permittivity value on the lens (center of the lens) is ε_r=6, decreasing continuously and smoothly to ε_r=2.25 on the edges, creating the desired permittivity profile (see Fig. 1). Consequently, we selected a Rogers TMM6 dielectric substrate (ε_r=6, tan δ=0.0023) with 7 mm of thickness, in order to fabricate the lens prototype. The different perforated dielectric flat lens characteristic parameters are summarized in Table I. The filling factor (α) is the fraction of area (or volume) of substrate material removed by the perforations to lower smoothly the permittivity from 6 to 2.25, depending on the diameter (d) and distance (s).

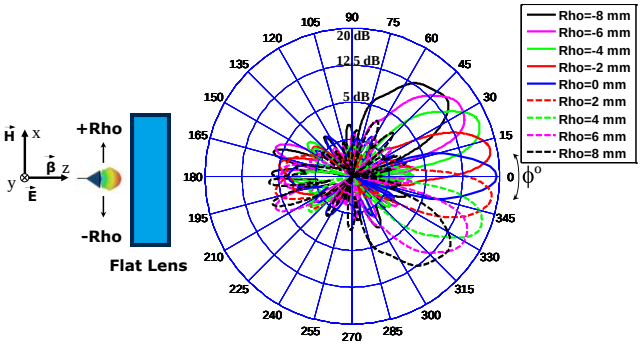

Fig. 2. H-Plane Gain (dB) Radiation Pattern CST simulation results at 60 GHz for each Rho feeding position.

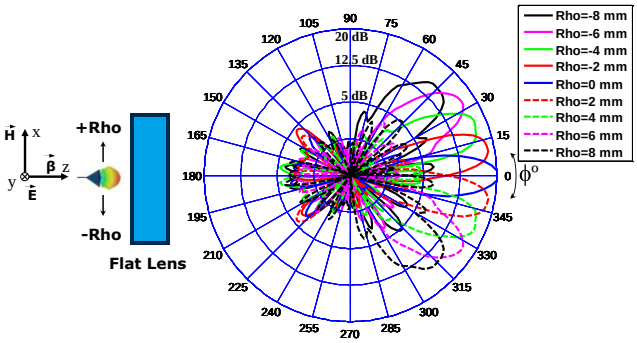

Fig. 3. H-Plane Gain (dB) Radiation Pattern CST simulation results at 77 GHz for each Rho feeding position.

B. Simulation Results

The perforated dielectric flat lens design has been simulated at 60 and 77 GHz using CST Microwave Studio with a time-domain solver in order to test its focusing capabilities [7],[10]. For each frequency, a total of 9 different simulations have been performed corresponding to different discrete positions of a radiating element (which could correspond to the positions of the antenna element in a switched-beam array) along the x-direction, going from Rho=-8 mm to Rho=+8 mm in steps of 2 mm (see Fig. 2 and Fig. 3). The radiating element used consists of a rectangular aperture (WR-15 waveguide for the 60 GHz setup and WR-10 waveguide for 77 GHz) with the E-field polarized in y-direction, which provides an efficient illumination of the lens with -14.8 dB edge taper in the H-plane.

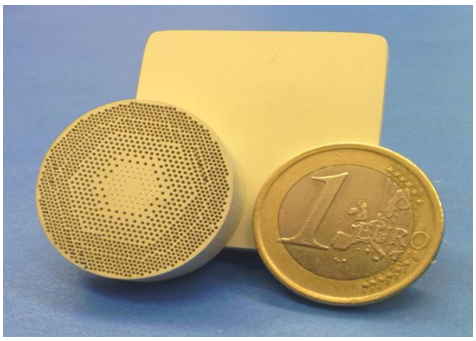

Fig. 4. Photograh of the fabricated dielectric flat lens prototype.

This article has been accepted for publication in a future issue of this journal, but has not been fully edited. Content may change prior to final publication. Citation information: DOI 10.1109/LAWP.2014.2363596, IEEE Antennas and Wireless Propagation Letters

Then, for each position of the waveguide, the corresponding H-plane radiation patterns are plotted at 60 GHz in Fig. 2, and at 77 GHz in Fig. 3.

III. Fabrication Process

A prototype of the designed perforated dielectric flat lens has been fabricated at UPC-AntennaLab facilities using a computer numerical control (CNC) machine. We performed a total of around 1200 holes on the TMM6 substrate with carbide drills of 0.2 and 0.5 mm of diameter to obtain the final lens prototype. A photograph of the lens is shown in Fig. 4.

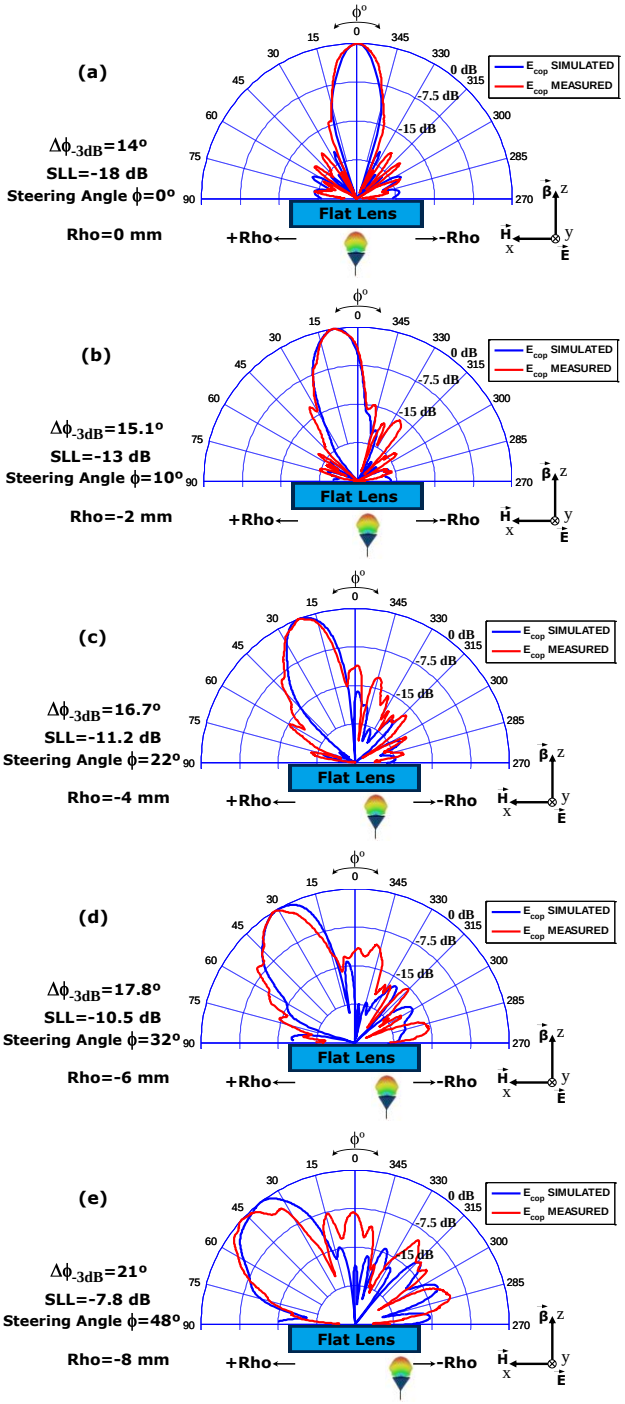

Fig. 5. Comparison between simulated and measured Normalized H-Plane Radiation Patterns at 60 GHz for different Rho feeding positions: (a) Rho = 0, (b) Rho=-2 mm, (c) Rho=-4 mm, (d) Rho=-6 mm, (e) Rho=-8 mm. Symmetric patterns steered rightwards are obtained for the symmetric feeding positions.

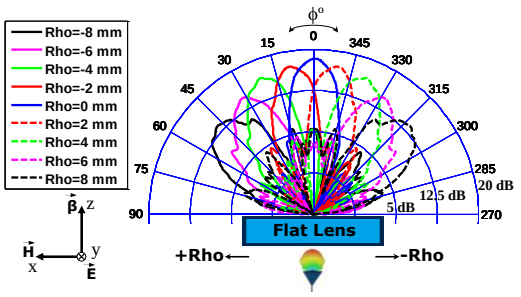

Fig. 6. Complete set of measured H-Plane Gain (dB) Radiation Patterns at 60 GHz for each Rho feeding position (from Rho=-8 mm to Rho=8 mm).

IV. Measurement Results

A complete set of measurements of the lens performance has been carried out at 60 GHz in the High Frequency Electronics laboratory of UCI, and at 77 GHz in the AntennaLab facilities of UPC. The radiation pattern produced by the lens has been measured at 60 GHz directly in the Far-Field using the measurement system of UCI. Since the highest frequency of the Far-Field measurement setup of UCI is 64 GHz, the E-Field radiated by the lens has been measured at 77 GHz in the Near-Field at AntennaLab facilities. Then, the Far-Field radiation pattern has been obtained at 77 GHz by using a Near-Field to Far-Field transformation [11].

A. *Measurement results at 60 GHz*

A total of 9 measurements have been performed corresponding to different feeding positions of the transmitting WR-15 waveguide along the x-direction (from Rho=-8 mm to Rho=8 mm) in steps of 2 mm. The WR-15 waveguide used during the measurements is well matched (S_{11} < -10 dB) for all the Rho feeding positions in the whole frequency band of interest. The corresponding H-plane radiation pattern results are shown in Fig. 5 (a-e). Given the lens structure, symmetric patterns are obtained for the corresponding symmetric feed positions with respect to the lens center, and therefore are not shown. As it is observed in Fig. 5(a-e), as the Rho feeding position is moved rightwards, the high-gain radiation pattern produced by the dielectric flat lens is steered leftwards, accordingly. In general, good agreement between radiation pattern simulation results and measurements at 60 GHz is observed.

In order to obtain the gain radiation pattern, we substitute the antenna under test (dielectric flat lens and the feeding WR-15 waveguide) for a well-known gain conical horn antenna (used as reference) to perform a received power level comparison. The complete set of gain radiation patterns for the 9 different Rho feeding positions is shown in Fig. 6. As it is observed, the measured gain values are very close to the simulation results (see Fig. 2). In addition, very good gain stability within the 60 GHz WPAN band (from 57 to 64 GHz) is

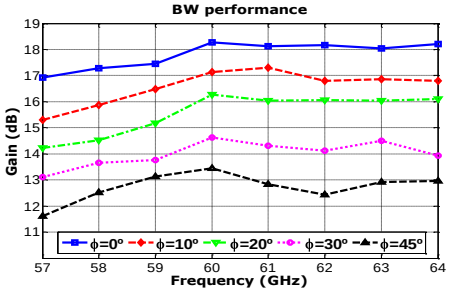

Fig. 7. Measured maximum gain (dB) for different ϕ focusing directions.

This article has been accepted for publication in a future issue of this journal, but has not been fully edited. Content may change prior to final publication. Citation information: DOI 10.1109/LAWP.2014.2363596, IEEE Antennas and Wireless Propagation Letters

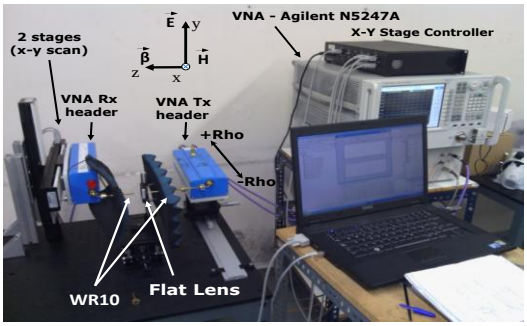

Fig. 8. 2D Near-Field measurement setup at 77 GHz.

observed from the measured bandwidth performance in Fig. 7. The measured radiation pattern parameters at 60 GHz (maximum gain for each beam, scan angles (Φ^o), half- power beamwidth ($\Delta\Phi_{-3dB}$), and SLL) are summarized in Table II.

B. Measurement results at 77 GHz

The 2D Near-Field measurement setup is shown in Fig. 8. It is composed of an Agilent N5247A vector network analyzer (VNA), two VNA extenders at W-band (one transmitter and one receiver), two precision linear stages to perform the 2D scan (X-Y movements), and two well-matched WR-10 open waveguides (one to feed the lens and one as a probe). RF absorbers are also used to avoid reflections between the instrumentation. The flat lens prototype is placed between the WR-10 waveguides. The transmitting WR-10 feeds the lens at its focal point (F=6.25 mm), and the receiving WR-10 is placed at 40 mm behind the lens to perform the 2D Near-Field measurement with the help of the 2 stages (see Fig. 8).

A total of 9 measurements have also been performed corresponding to different feeding positions of the transmitting WR-10 along the x-direction. The corresponding H-plane radiation pattern results have been obtained. In addition, gain measurements have also been performed at 77 GHz; we also substitute the antenna under test for a well-known gain conical horn antenna to perform a received power level comparison, after the Near-Field to Far-Field transformation of the measurements [11]. The complete set of gain radiation patterns for the 9 different Rho feeding positions is shown in Fig. 9, and the radiation pattern parameters at 77 GHz are also summarized in Table II. In the last case (Rho=±8 mm), the SLL is not much lower because of the diffraction on the lens edges and it could be considered not acceptable. Moreover, because we are using an open-ended wave-guide to illuminate the lens, there can be spurious radiations, which affect the SLL and the maximum achievable gain. In this sense, an optimum radiating element has to be designed for an optimum lens illumination for high steering angles. As at 60 GHz, good

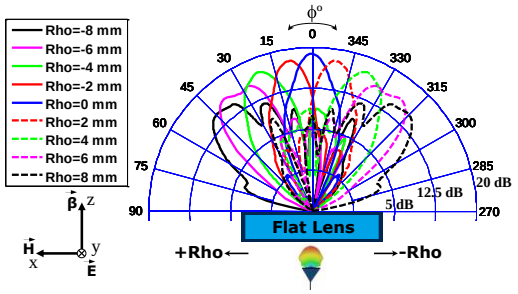

Fig. 9. Complete set of measured H-Plane Gain (dB) Radiation Patterns at 77 GHz for each Rho feeding position (from Rho=-8 mm to Rho=8 mm).

TABLE II. SUMMARY OF FLAT LENS PERFORMANCE AT 60 AN 77 GHZ

Feeding Position (Rho)	PERFORMANCE AT 60 GHz				PERFORMANCE AT 77 GHz			
	Gain	(ϕ^o)scan	$\Delta\phi_{-3dB}$	SLL	Gain	(ϕ^o)scan	$\Delta\phi_{-3dB}$	SLL
0 mm	18.3 dB	0º	14º	-18 dB	18.9 dB	0º	12º	-20 dB
±2 mm	17.2 dB	±10º	15.1º	-13 dB	17.8 dB	±9.8º	13º	-14 dB
±4 mm	16.6 dB	±22º	16.7º	-11.2 dB	17.3 dB	±21.6º	16.3º	-8.2 dB
±6 mm	14.7 dB	±32º	17.8º	-10.5 dB	16.5 dB	±37.5º	24º	-8.9 dB
±8 mm	13.7 dB	±48º	21º	-7,8 dB	15.4 dB	±44.2º	20º	-3.5 dB

agreement between radiation pattern simulation results and measurements is also observed at 77 GHz (see Fig. 3 and Fig. 9). Note that we cannot obtain the directivity (or the efficiency) of the dielectric flat lens antenna with our 2D Near-Field measurement setup since there is a part of back radiation, due to the reflections on the lens, that cannot be measured. Therefore, we estimated the loss efficiency using the gain measurements and CST simulation results of the directivity, obtaining very good values between 70% and 80% at both frequency bands as a low loss substrate is used.

V. CONCLUSIONS

In this paper we have presented a novel inhomogeneous gradient-index dielectric flat lens antenna for millimeter-wave applications. Its performance has been evaluated at 60 and 77 GHz. Measurements at both frequencies indicate that we can achieve beam-steering capabilities in both planes from -30º to +30º with around 17 dB of gain and low side-lobe levels, and up to ±45º with around 15 dB of gain. It has been practically demonstrated that this design could be used to develop a complete switched-beam array for millimeter-wave systems, including high throughput communications at 60 GHz for WPAN applications and automotive radar systems at 77 GHz, due to its high-gain and beam-steering capabilities. The proposed antenna solution represents an interesting alternative to the existing antenna configurations at millimeter wave frequencies above 60 GHz to achieve beam-scanning in both planes, broadband operation, and flat antenna profile.

REFERENCES

[1] R. Fisher, "60 GHz WPAN standardization within IEEE802.15.3c," in *Proc. Int. Signals, Syst. Electron. Symp.*, 2007, pp. 103-105.

[2] T.S. Rappaport, J.N. Murdock, and F. Gutierrez, "State of the art in 60-GHz integrated circuits and systems for wireless communications," *Proc. IEEE*, vol.99, no. 8, pp.1390-1436, Aug. 2011.

[3] W. Menzel and A. Moebius, "Antenna concepts for millimeter-wave automotive radar sensors," *Proc. IEEE*, vol. 100, no.7, pp.2372-2379, Jul. 2012.

[4] M. Imbert, J. Romeu, and L. Jofre, "Design of a dielectric flat lens antenna for 60 GHz WPAN applications," in *Proc. IEEE Antennas and Propag. Society Int. Symp.*, Orlando, FL, Jul. 2013, pp. 1164-1165.

[5] A. Petosa, and A. Ittipiboon, "Design and performance of a perforated dielectric fresnel lens," *IEE Proc.-Microw. Antennas Propag.*, vol. 150, no. 5, pp. 309-314, Oct. 2003.

[6] G. Peeler, and H.P. Coleman, "Microwave stepped-index Luneberg lenses," *IEEE Trans. Antennas Propag.*, Vol. 6, No. 2, 202-207, 1958.

[7] B. Fuchs, O. Lafond, S. Palud, L. Le Coq, M. Himdi, M. C. Buck, and S. Rondineau, "Comparative design and analysis of Luneburg and half maxwell fish-eye lens antennas," *IEEE Trans. Antennas Propag.*, vol. 56, no. 9, pp. 3058–3062, Sep. 2008.

[8] K. Sato, and H. Ujiie "A plate Luneberg lens with the permittivity distribution controlled by hole density," *Electron. Commun. Jpn*. vol. 85, no. 9, pt. Part 1, pp. 1–12, 2002.

[9] B. Zhou, Y. Yang, H. Li, and T. J. Cui, "Beam-steering Vivaldi antenna based on partial Luneburg lens constructed with composite materials," *Journal of Applied Physics*, Vol. 110, 084908(6), 2011.

[10] Y. Zhang; W. Hong; Y. Zhang "A beam steerable plane dielectric lens antenna," in *Proc. Int. Symp. on Antennas and Propag. (ISAP), 2013*, vol.01, no., pp.476,479, 23-25 Oct. 2013.

[11] A.D. Yaghjian, "An overview of near-field antenna measurements," *IEEE Trans. Antennas Propag.*, vol. AP-34, no. 1, pp. 30–45, Jan. 1986.